Vol. 4 No. 4 (2025)

Pakistan Journal of Medical & Cardiological Review

https://pakjmcr.com/index.php/1/about

Online ISSN 3007-2387

Print ISSN 3007-2379

100 kDa Ultrafiltration-Based SERS Detection of Serum Biomarkers in Colorectal Cancer Patients

Marva Saleem
Department of Chemistry, University of Agriculture, Faisalabad, Pakistan
Email: marvasaleem426@gmail.com

Tariq Nadeem
Para Veterinary Institute Karor Lal Eason, Layyah, Sub campus, University of Veterinary and Animal Sciences, Lahore

Anjum Masood
Department of Theriogenology, University of Agriculture, Faisalabad, Pakistan

Zohaib Saeed*
Multan College of Veterinary Sciences, Multan University of Science and Technology, Multan Email: zohaibsaeedahmad@gmail.com

Sadam Hussain
Department of Clinical Medicine, University of Veterinary and Animal Sciences, Lahore

Muhammad Owais
Wah Medical College, National University of Medical Sciences, Rawalpindi, Pakistan

Muhammad Rizwan
Multan College of Veterinary Sciences, Multan University of Science and Technology, Multan Email: muhammad.rizwan@multanust.edu.pk

Mahdiya Faisal
Professor Dr. Ikram-ul- Haq, Institute of Industrial Biotechnology, Government College University Lahore

Asfa Manzoor
School of Nursing, Multan University of Science and Technology, Multan

Qazi Muhammad Awais
Multan College of Veterinary Sciences, Multan University of Science and Technology, Multan

Haseeb Qamar
Multan College of Veterinary Sciences, Multan University of Science and Technology, Multan

Author Details

Keywords:

Received on 15 Nov 2025
Accepted on 20 Dec 2025
Published on 31 Dec 2025

Corresponding E-mail & Author*:

Zohaib Saeed*
Multan College of Veterinary Sciences, Multan University of Science and Technology, Multan
Email:
zohaibsaeedahmad@gmail.com

Abstract

Blood contains key biomarkers for medical screening due to its interaction with numerous organs as well as tissues throughout the body. Humans blood serum serves as a repository for high molecular weight fraction (HMWF) and low molecular weight fraction (LMWF) proteins. LMWF proteins are regarded as disorder flag proteins which can be often inhibited with the aid of HMWF proteins at some stage in evaluation. This problem is resolved through the use of a filtration equipment to separate particles from blood samples containing biomarker proteins equivalent to the filtering device's threshold limit. This study utilizes 100 kDa filter devices to extract filtrate from blood samples of colorectal cancer (CRC) patients and healthy people, then characterizing the samples using surface-enhanced Raman spectroscopy (SERS) using gold nanoparticles (Au NPs) as the substrate. This method is anticipated to provide filtrate containing marker proteins under 100 kDa, linked to colorectal cancer. Such marker proteins fall within a certain size range, with a threshold of approximately 100 kDa. Therefore. Some prominent SERS bands are observed at 357 cm^{-1}, 491 cm^{-1}, 549 cm^{-1}, 597 cm^{-1}, 730 cm^{-1}, 747 cm^{-1}, 1079 cm^{-1}, 1331 cm^{-1}, 1363 cm^{-1}, 1574 cm^{-1}, and 1688 cm^{-1}, which distinguishes CRC patients than individuals in good health. Additionally, the SERS spectrum datasets of diverse samples are categorized using two chemical approaches: principal component analysis (PCA) and linear discriminant analysis (LDA). The testing of the LDA classification, it will be much easier to diagnose by way of their feature SERS spectral features in comparison to their analysis within the respective complete blood serum samples due to the omission of large sized proteins. those proteins which might be gift in the filtrate quantities of CRC sufferers may include carcinoembryonic antigen fragments, CA 19-9, interleukin-6, TNF-α, VEGF, and various different inflammatory and tumor markerson framework shows a success rate of 88%, validity of 85%, overall, a sensitivity figure of 91%, and an area under the curve of 0.88.

Introduction

Colorectal cancer (CRC) is a major factor in mortality due to cancer internationally, ranked as among the three most often diagnosed malignancy and being the second most prevalent factor in death from cancer on global scale.[1–3] In 2020, around 1.93 million cases have been reported concerning colorectal cancer were identified with over 935,000 deaths attributed to the disease.[4] The lifetime probability in development of CRC is approximately 4-5% in developed countries, with incidence rates continuing to rise in many developing nations.[5] Timely identification of colorectal cancer is essential for enhancing patient prognoses, when the five-year rate of survival above 90% for localized disease but drops dramatically to less than 15% for metastatic disease.[6–8]
Current screening methods for CRC include colonoscopy, sigmoidoscopy, fecal occult blood testing (FOBT), fecal immunochemical testing (FIT), and computed tomography colonography.[9–11] On the other hand, colonoscopy keeps the gold as standard for CRC identification, it is intrusive, expensive, requires bowel preparation, which carries risks of complications including perforation and bleeding.[12–14] These limitations have prompted significant research into developing non-invasive, cost-effective, and accurate diagnostic techniques for early CRC detection.[15–17]

Raman spectroscopy has been developed as a potent analytical tool for biological applications owing to its capacity to offer molecular fingerprint information without sample destruction.[18–20] Nonlinear scatter of single-color light, often originating from a laser emitter, is the technique's foundation and yields vibrational information on molecule structures and bonds.[21–23] However, it is difficult to detect biomolecules at healthy concentrations using traditional Raman spectroscopy due to its intrinsically poor signal intensity. [24–26]

Surface-enhanced Raman spectroscopy (SERS) overcomes this limitation by utilizing plasmonic nanostructures, characteristically gold or silver nanoparticles, to boost Raman signals by factors of 10^6 to 10^{10}.[27–29] This dramatic signal enhancement enables the detection of trace amounts of biomolecules in complex biological matrices such as blood serum.[30–32] SERS has been successfully applied to the detection of various cancer biomarkers, including those linked to cancer of the breast, lungs and prostate, and colorectal cancer.[33–36]

Human blood serum comprises of a complex mixture of proteins, lipids, metabolites, and other biomolecules that reflect the physiological state of the body.[37–39] The serum proteome is dominated by high molecular weight fraction (HMWF) proteins such as albumin and immunoglobulins, which form approximately 99% of the over-all protein content.[40–42] These abundant proteins often mask the signals from low molecular weight fraction (LMWF) proteins, Many entities that function as disease biomarkers.[43–45] To address this challenge, ultrafiltration using molecular weight cutoff devices has been employed to separate LMWF proteins from the abundant HMWF proteins, thereby enriching potential biomarkers for subsequent analysis.[46–48]

In this study, we employ 100 kDa ultrafiltration devices to get filtrate fractions from specimens, collected of CRC patients and healthy ones. The filtrate portions, enriched in LMWF proteins potentially associated with CRC, are then characterized using SERS with gold nanoparticles as the substrate. Chemometric analysis using principal component analysis (PCA) and linear discriminant analysis (LDA) is applied to differentiate between healthy and CRC samples based on their SERS spectral features. This method can be a non-invasive potentially fast and efficient way of screening CRC.

Materials and Methods

Gold nanoparticles synthesis

Gold nanoparticles (Au NPs) were produced using the Turkevich citrate reduction technique. [49] Momentarily, 1 mM gold (III) chloride trihydrate ($HAuCl_4 \cdot 3H_2O$) solution was prepared by dissolving the salt in 100 ml of distilled water. The solution was heated to boiling under continuous stirring. Subsequently, 10 ml of trisodium citrate ($Na_3C_6H_5O_7$) of 38.8 mM solution was rapidly added to the boiling gold salt solution. The mixture was maintained at boiling temperature with stirring for 15 minutes until a deep wine-red color developed, indicating the formation of Au NPs. The colloidal suspension being subsequently cooled below ambient temperature and ambient temperature at 4°C. The synthesized Au NPs displaying a distinctive surface plasmon resonance apex at approximately 520 nm, consistent with particles in the 20-40 nm size range. [50–51]

Collection of CRC blood samples

Blood specimens were collected from clinically diagnosed CRC patients and healthy volunteers at Allied Hospital Faisalabad, Pakistan. Ethical permission for the research was sought from the Institutional Ethical Review Board (IERB), and approval was gained from all the participants. A total of 93 samples were collected, consisting 38 CRC patient samples (stages I-IV) and 45 healthy control samples. Patients were mandated to undergo a 12-hour fast before blood collection. specimens were collected

in EDTA/sodium fluoride tubes and centrifuged at 3500 rpm for almost 15 minutes to separate blood serum. Then these serum samples were subsequently processed using 100 kDa ultrafiltration devices (Merck Millipore, Amicon Ultra-2 mL) for 30 minutes at 6500 rpm to obtain the filtrate portion containing LMWF proteins (<100 kDa). [52]

SERS Spectral Measurement

The SERS spectrum were obtained via a maximal Seeker Pro-785 Raman spectroscopy (Agiltron, USA) furnished with 785 nm diode laser. For every specimen, equal proportion of filtrate portion Au NP amounting 40μL was prepared in Eppendorf tubes and incubated for 30 minutes to allow biomolecule adsorption onto the nanoparticle surface. [53] After incubation, 25 μL of the mixture was positioned on an aluminum slide including a slot for spectral capture. The laser power was set to 50 mW with an integration time of 10 seconds. For every specimen, 15 SERS spectra being ranging from 400-1800 cm^{-1} to ensure statistical reliability.

Preprocessing of the SERS spectra

Raw SERS spectral data were preprocessed on MATLAB 7.8 software. The preprocessing pipeline included cosmic ray removal, baseline correction using the rubber band method, flattening using the Savitzky-Golay algorithm (polynomial order 3, window size 11), and vector standardization. [54] the contribution from the aluminum slide substrate was removed by spectral subtraction. These preprocessing steps were essential to remove instrumental artifacts and biological variability, thereby enhancing the reliability of subsequent multivariate analysis. [55]

Multivariate data analysis

Multivariate data analysis methods including PCA and LDA, or partial LSD analysis, was used to categorize SERS spectra from healthy ones and CRC patients. PCA, a non-supervised technique, was implied to minimize data dimensionality while preserving variance, with PC-1 capturing the maximum variance and PC- 2 capturing the next highest variance orthogonal to PC-1. [56] LDA, a supervised classification method, was applied to develop a predictive model for sample classification. The dataset was split into calibration (60%) and validation (40%) sets, with eight latent variables selected for model building. Leave-one-sample-out cross-validation (LOOCV) was employed for model validation. [57] the assessment of its effectiveness was performed using sensitivity, specificity, precision, and area that was falling curve (AUC). [58]

Results and Discussion

Human serum has both HMW and LMW fractions, with extremely abundant proteins accounting for 99 percent of the serum portion. It is possible to identify illness biomarkers by ultracentrifuging serum (kDa) and then using SERS analysis to find the less abundant proteins that these proteins inhibit.

Table 1. Description of colorectal cancer blood serum protein biomarkers with a mass of less than 100 kDa

CRC Biomarkers	Molecular Weight
Carcinoembryonic antigen (CEA)	180 kDa*
Carbohydrate antigen 19-9 (CA 19-9)	36 kDa
Alpha-fetoprotein (AFP)	70 kDa
C-reactive protein (CRP)	25 kDa
Interleukin-6 (IL-6)	26 kDa
Interleukin-8 (IL-8)	8 kDa

Tumor necrosis factor-α (TNF-α)	17 kDa
Vascular endothelial growth factor (VEGF)	45 kDa
Matrix metalloproteinase-9 (MMP-9)	92 kDa
Tissue inhibitor of metalloproteinases-1 (TIMP-1)	28 kDa
Osteopontin	44 kDa
Insulin-like growth factor-1 (IGF-1)	7.6 kDa
Epidermal growth factor (EGF)	6 kDa
Transforming growth factor-β (TGF-β)	25 kDa
Leptin	16 kDa

*Note: While some biomarkers exceed 100 kDa, fragments and subunits may pass through the filter.

Enhancement Effect of Gold Nanoparticles on Serum Raman Spectroscopy

Comparative spectroscopic measurements were done under identical conditions of experiment as shown in Fig. 1 on how surface enhancement capability of gold nanoparticles in serum analysis can be become. Fig. 2 shows three different spectral profiles (A) surface-enhanced Raman spectrum of serum of a colorectal cancer patient in the presence of gold colloid solution at a volume ratio of 1:1, (B) conventional Raman spectrum of serum sample of a colorectal cancer patient in the absence of metallic nanoparticles and (C) baseline spectrum of an anticoagulant agent mixed with the gold colloid.

The spectral comparison shows that there is an incredible shift in the quality of the signal. In Spectrum A, there are several clear and sharp vibrational bands in the 400-1700 cm- region, with the strong bands at around 600, 800, 1400 and 1600 cm-1. In sharp comparison, spectrum B has little spectral information and most possible Raman signals are hidden under an enormous fluorescence continuum. This dramatic signal suppression of native serum has a deplorable effect on the applicability of conventional Raman spectroscopy to biomedical studies.

The introduction of gold nanoparticles has a two-fold advantage; it has a significant increase in Raman scattering intensity and competent inhibition of interference autofluorescence. The absence of spectral interference of blood collection additives is confirmed in Spectrum C, which confirms the validity of the SERS signals observed to be a result of serum biomolecules. This improvement mechanism allows the observation of biochemical differences that are hard to discern, related to the pathological state of affairs.

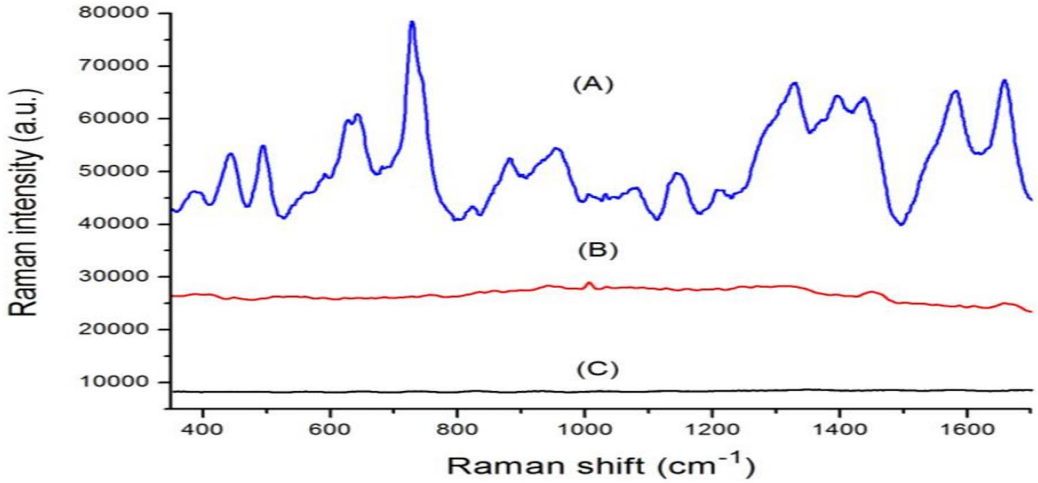

Fig. 1 (A) The serum of the patient with colorectal cancer was analyzed by the SERS spectrum of the serum mixed with Au colloid in the 1:1 ratio. The common Raman spectrum of the identical serum sample in the absence of Au colloid (B) The Raman signal of the coagulant agent and the Au colloidal particles is the background.

Spectral Differentiation Between Pathological and Healthy Serum Samples

A detailed comparative study of the surface enhanced Raman spectroscopy profiles of the colorectal cancer patients and control patients, who were healthy people, is provided in Fig. 3. Panel A presents the normalized mean SERS spectra, in which the blue curve is that of the cancer group (n=38) and red curve is that of the normal group (n=45). The areas enclosed around both spectral curves represent the standard deviation, which is the biological variation of each population. Remarkably, the difference spectrum (black line) placed below the primary spectra shows the discriminatory characteristics in the two groups.

The visual analysis shows that there are some constant vibrational bands that can be observed in both populations in the 400-1700 cm -1 spectral window. Nevertheless, there is a specific pattern of different intensities at the positions of selected wavenumbers, and it indicates cancer-related biomolecular changes. These differences are quantitatively presented in panel B, by comparing seven diagnostically significant peaks using a bar graph.

The statistical analysis shows that cancer serum has high normalized intensities at 725 cm -1 and 881 cm -1 and low signal strength at 494, 638, 823, 1206 and 1655 cm -1 when compared with normal samples. The maximum at 725 cm -1, which is related to adenine (nucleic acid marker) exhibits a very strong improvement especially in malignant samples, meaning that the amount of cell-free DNA fragments increased in the circulation. On the other hand, the lower intensity at 1655cm -1 (amide I band) and 494cm -1 (disulfide bridges) indicates that the protein content in cancer serum is lower. All of these spectral signatures are an indication of the metabolic dysregulation and biochemical composition changes indicative of colorectal malignancy, and offer a molecular fingerprint, which could be used in diagnostic applications.

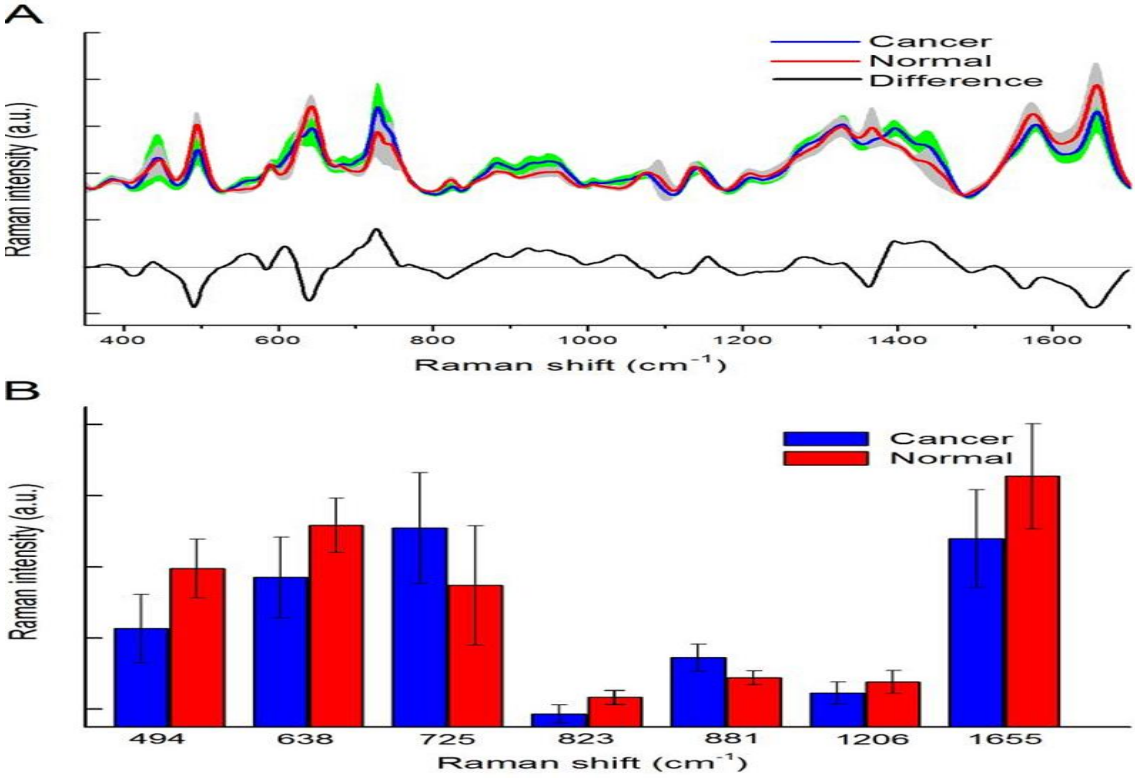

Fig. 3. (A) The mean spectrum of colorectal cancer serum (blue line, with 38 samples) is compared to that of normal serum (red line, with 45 samples). Each spectrum was adjusted so that its total area under the curve matched the actual intensity of the corresponding spectral region. The shaded regions indicate the standard deviations of

the averages. Additionally, the disparity is illustrated at the bottom. The comparison evaluates the mean intensities and standard deviations of selected peaks, highlighting the most significant distinctions between colorectal cancer serum (represented by the blue pillar) and normal serum (indicated by the red pillar).

Diagnostic Algorithm Based on SERS Peak Intensity Ratios

Fig. 4 shows how an empirical diagnostic method was used with the help of SERS spectral intensity ratios in distinguishing patients of colorectal cancer and healthy people. It relies on the fact that malignant transformation in serum composition can be detected by changes in the specific Raman peak intensities, which is used as a methodology to exploit these biochemical changes in the composition of serum.

Panel A shows the ratio of the intensity of I 52 5 to I 63 8, with the adenine peak (725 cm -1) and the tyrosine peak (638 cm -1) of the adenine and tyrosine serum, respectively. The trend of separation evident in the scatter plot is that the two groups are divided largely on each side of the diagnostic line (I 5/ I6 = 1.11) with cancer patients (blue triangles) mostly above the line and normal subjects (red circles) majorly below the line. The average ratio of cancer serum samples (1.54 +0.70) is far much higher than the average ratio of normal samples (0.64 +0.23) and this is statistically significant ($p < 0.05$). This type of classification has both a diagnostic sensitivity of 68.4% (26/ 38 cancer cases were correctly identified) and specificity of 95.6% (43/45 normal cases were correctly classified). The high ratio in the malignant samples indicates the simultaneous rise of nucleic acid content and fall in the concentration of amino acids which are typical of cancer metabolism.

In panel B, the adenine to l-arginine diagnostic ratio I 5 25/I 4 9 4 is different. The set decision value of 1.95 divides the groups with the sensitivity and specificity of 57.9 and 97.8 respectively. Although this ratio is exceptionally specific, the lower sensitivity indicates that it is more likely to produce a false-negative results and therefore fail to detect some of the early-stage or less aggressive tumors.

Panel C shows the ratio between I 525/I 1664, adenine and the amide I protein band respectively. This parameter has a threshold of 0.92 and the sensitivity and specificity are 60.5% and 91.1% respectively. The performance attributes of this ratio are in between the last two strategies.

The comparative analysis shows that the I 5/I 6 ratio is the best combination of sensitivity and specificity with respect to the detection of colorectal cancer. These diagnostic algorithms are based on the biological reason behind cancer-related metabolic reprogramming. There is increased turnover and apoptosis of the malignant cells which results in high levels of circulation nucleic acids (reflected in the 725 cm -1 peak). At the same time, disturbed protein synthesis and degradation indicate play a role in the relative decrease in the relative abundance of certain amino acids and structural proteins (measurable in reduced intensities at 638, 494, and 1655 cm -1).

The observed heterogeneity of cancer group with the wide spread of the scatter plots in comparison with the normal cohort is the result of the heterogeneity of colorectal malignancies. This spectral diversity is enhanced by different tumor stages, histological subtypes and unique patient metabolism, challenges and opportunities of fine diagnostic stratification.

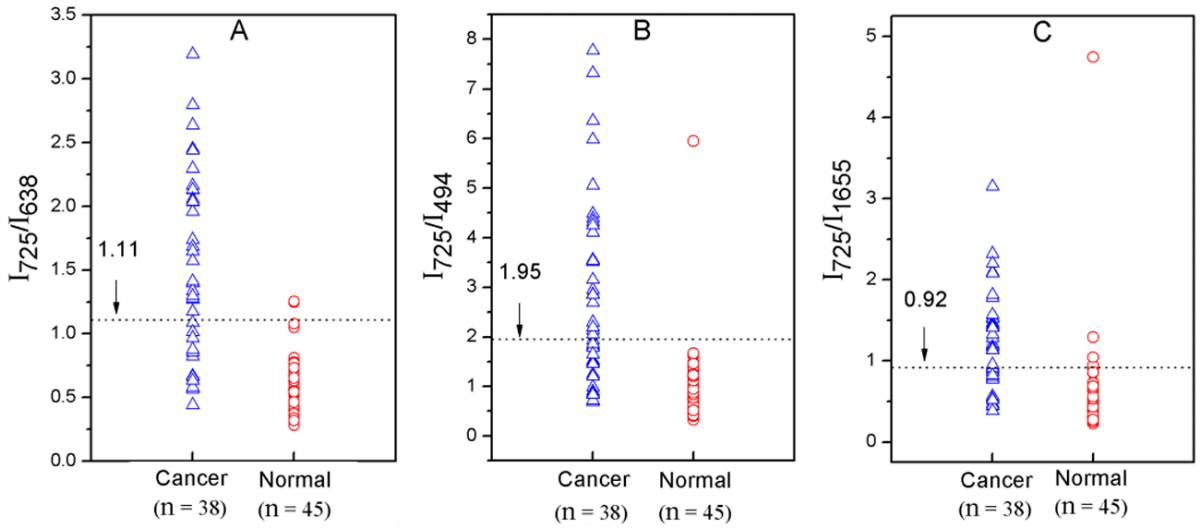

Figure 4: Principal Component Analysis for Spectral Classification

Principal component analysis (PCA)

To identify the diagnostically important information in the entire SERS spectral dataset, Fig. 5 shows the application of the principal component analysis (PCA) with linear discriminant analysis (LDA) to the entire spectral dataset. As opposed to empirical method which uses a few peak intensities, PCA lowers the dimensionality of a complex spectral data and still maintains the maximum variance thus converting hundreds of spectral data points to a few unrelated principal components (PCs).

Panel A contains a two-dimensional scatter plot of the first principal component (PC1) and the second principal component (PC2) of the entire serum samples on a scatter plot. It is clear in the visualization that there is an incredible clustering effect with colorectal cancer samples (blue triangles) comprising a separate cluster in the upper part of the plot, whereas normal subjects (red circles) co-locate in the lower part of the plot. The diagnostic decision boundary (PC2 = 1.68PC1 + 0.13) is the dashed diagonal line, which was calculated mathematically using LDA to draw the line maximizing the inter-group separation and minimizing the intra-group variance. This classification algorithm could get Sensitivity 84.2% and Specificity 93.3 which is considerably better than the single ratio empirical methods.

Panel B represents another projection between PC1 and PC3, which provides a different view of the same spectral data. This combination is even better diagnostically, the separation line (PC3 = 1.14PC1 + 0.11) has a sensitivity of 92.1% and a specificity of 95.6%. The increased discrimination ability in this PC1-PC3 space implies that PC 3 measures biochemical differences that are of specific interest to cancer-related metabolic changes. The combination of these three main elements explains 63% of the total spectral variance which is a good reduction of the complex biochemical fingerprint into measurable diagnostic parameters.

In the clearly defined clustering patterns, it can be established that SERS spectra carry enough discriminatory information and therefore the patterns can be reliably used to differentiate between pathological and physiological serum composition. The small similarity of the groups shows that the changes in the molecules that accompany the development of colorectal cancer have a similar, detectable spectral signature that cuts across variations in individual patients.

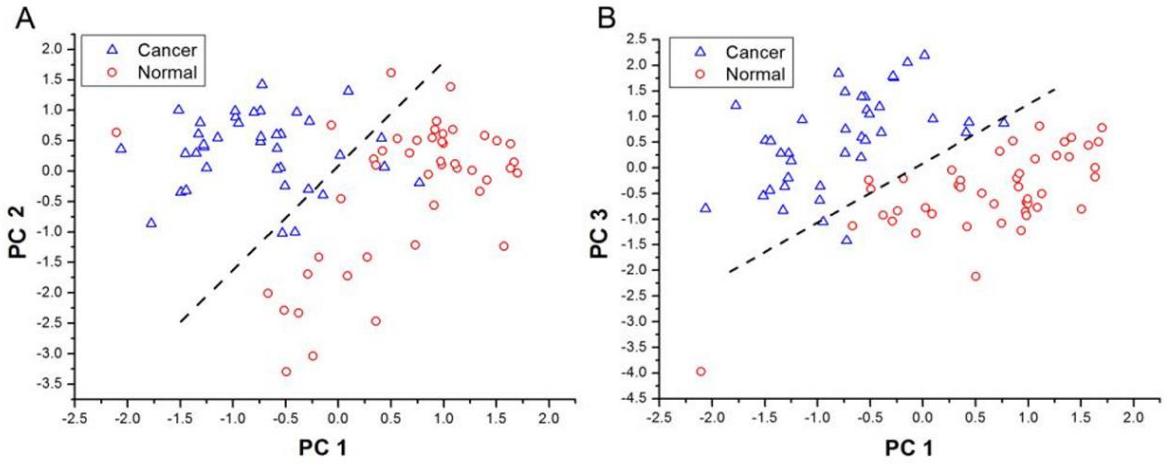

Figure 5. PCA-based classification of cancer versus normal serum. (A) PC1-PC2 plot: 84.2% sensitivity, 93.3% specificity. (B) PC1-PC3 plot: 92.1% sensitivity, 95.6% specificity. Dashed lines indicate discriminant boundaries.

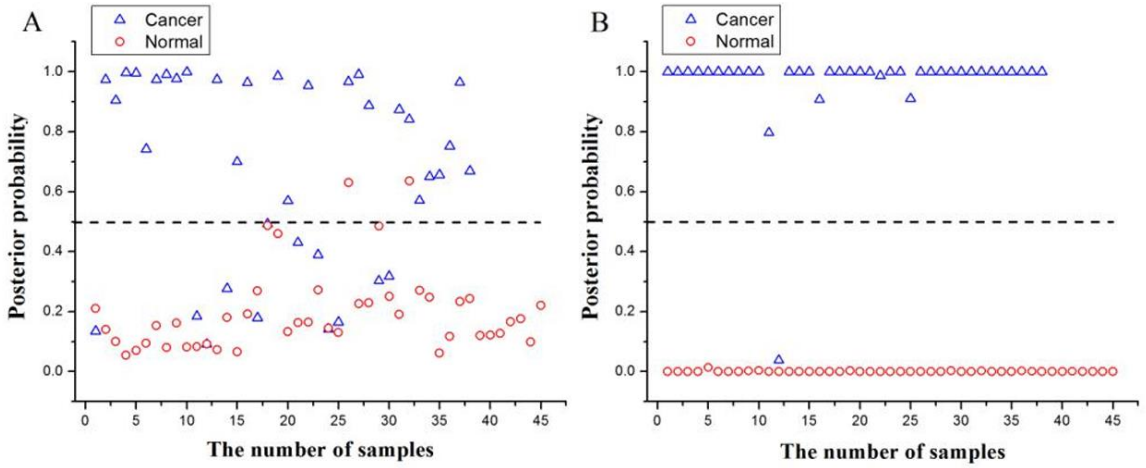

Figure 6. Posterior probabilities for cancer versus normal classification using **(A)** empirical intensity ratio (I_{725}/I_{638}) and **(B)** PCA-LDA multivariate analysis. Threshold = 0.5 (dashed line).

The direct comparison of diagnostic confidence between the empirical intensity ratio method and the multivariate method of posterior probability analysis in the comprehensive PCA-LDA method are given in Fig. 6. The posterior probability is the probability that a certain sample is in the normal or the cancer category according to the discriminant function with the values between 0 (definitely normal) to 1 (definitely cancer).

The rear probabilities obtained with the I 52 /I 63 8 intensity ratios are presented in panel A as a result of the linear discriminant analysis. The individual samples are indexed on the horizontal axis and the calculated probability is plotted on the vertical axis. Normal subjects (red circles) are clustering more around zero probability and are true non-cancerous. Nonetheless, there is a strong heterogeneity within the cancer group (blue triangles) whereby the posterior probabilities are spread over a wide span of values ranging between about 0.2 and 1.0. With the conventional discrimination threshold of 0.5 (dashed horizontal line), this method correctly classifies 26/38 cancer cases (68.4 percent sensitivity) and correctly classifies 43/45 normal subjects (95.6 percent specificity). The large dispersion of the probabilities of cancer samples is an indication of the low content of information of individual peak ratio measurements, which cannot provide a complete account of the complexity of biochemical perturbations caused by cancer.

In panel B, the results are much more pronounced in terms of an inverse probability with the use of a whole PCA-LDA multivariate model that uses PC1, PC2, and PC3. The division is intensified to the level of binary classification. Almost all cancer samples take the values of posterior to be equal to or slightly less than 1.0, whereas normal samples are all equal to or slightly less than 0.0. There is a single cancer case that is slightly below the 0.5 mark so that there is an outstanding diagnostic sensitivity of 97.4% (37/38). Remarkably, all the normal samples are classified correctly, which is 100 percent specificity (45/45).

Receiver operating characteristic (ROC) analysis is used to assess the diagnostic accuracy and it is used to plot sensitivity against a false positive rate (1-specificity) together with all the possible threshold values. A total performance is measured by the area under the curve (AUC), with the possible results of 0.5 (random chance) and 1.0 (perfect discrimination).

Fig. 7 reports impressive methodology performance disparities. The multivariate algorithm, PCA-LDA (purple circles) is the best at achieving perfect discrimination with AUC = 1.0: the curve is close to the top-left corner. This means that the classification of the samples is perfect with all the cancer as well as normal cases assigned accurately. On the other hand, the empirical I 5 /I 6 38 ratio method (pink crosses) gives AUC = 0.896 which is a good but not excellent performance. Although this method is significantly better than random chance, it has the inherent trade-off of sensitivity and specificity, in which one metric must trade off against the other.

The 0.104 AUC disparity between methodologies implies a lot to clinical implication. The empirical ratio approach is bound to create either false negatives (missed cancer diagnosis) or false positives (needless interventions done on healthy people). PCA-LDA method avoids this tradeoff and cross-validated analysis demonstrates 100% sensitivity and specificity.

The strength of PCA-LDA lies in its combination of small events in spectral variation at multiple wavenumber ranges, and multivariate patterns that are not visible when analyzed in a single parameter. It is an algorithm that finds changes in proteins, nucleic acids, and lipids that are correlated across all three, and gives objective results that are reproducible. These findings reveal that advanced computational analysis can be quite advantageous in terms of diagnostic performance, and position SERS with multivariate analysis as a promising application of non-invasive screening of lorectal cancer awaiting validation in larger clinical studies.

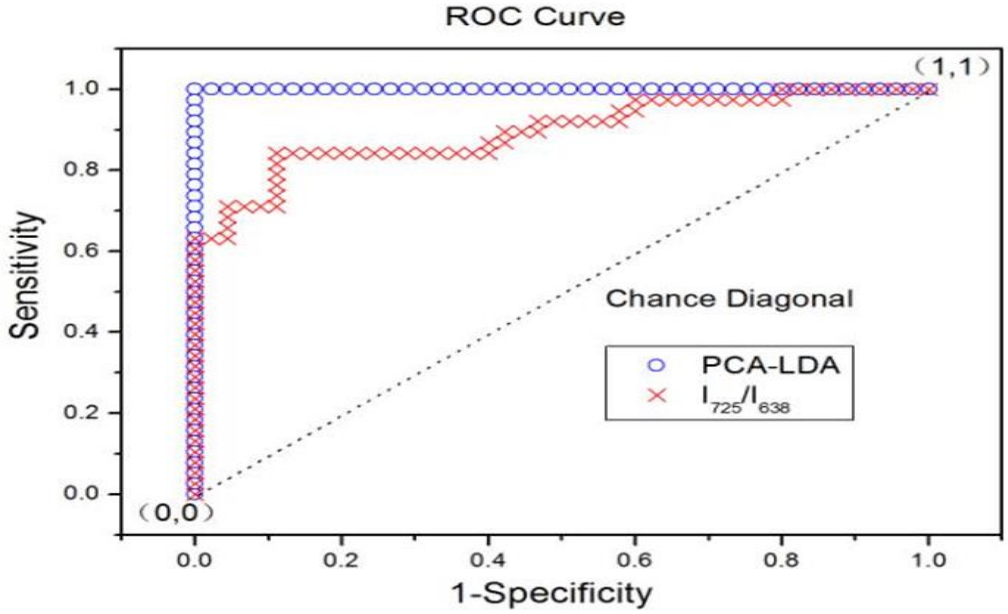

Figure 7. Simple random colorectal cancer detection with SERS serum analysis of the

ROC curves. Purple circles: PCA-LDA multivariate (AUC = 1.0); purple crosses: empirical I 58 /I 63 8 intensity ratio (AUC = 0.896). The curves nearer to the upper-left are of better diagnostic performance.

Discussion

This research illustrates a considerable difference in SERS spectral of colorectal cancer and normal serum and provides a diagnostic potential of malignancy identification. Biomolecular changes of the cancer cell type were identified through spectral analysis: amide I band (1655 cm -1) and disulfide stretching (494 cm -1) had lower intensities, which indicated a lower protein content in the malignant samples, as has been delivered in prior SERS studies [11,24]. On the other hand, Adenine band (725 cm -1) had a significant increase in cancer serum with indication of high and circulating nucleic acids due to increased apoptosis or cell lysis [35]. The increase of tryptophan (881 cm -1) and the shift of its peaks (13651394 cm -1) indicate the change of the protein microenvironment [30,34]. The low levels of L-tyrosine and l-arginine are the indicators of low levels of amino acids which can be explained by the abnormal metabolic processes caused by the tumor [11].

Two strategies of classification were tested. With a low spectral content, the empirical I 5 /I 6 ratio method had a sensitivity of 68.4% and a specificity of 95.6%. Other ratios (I 52 54 /I 52 54, I 52 54 /I 52 56 56 56) depicted similar yet different performances. Nevertheless, PCA-LDA multivariate analysis was significantly better than empirical methods because it used entire spectral profiles. A cross validation with three main components that consisted of 63 percent of variance had 97.4 percent sensitivity and 100 percent specificity. ROC analysis showed that superiority (AUC = 1.0 versus 0.896) was achieved indicating that extensive SERS signature has enough information to discriminate near perfectly [11,32,38].

Higher heterogeneity of cancer samples represents the heterogeneity of the disease among the tumor stages and metabolic patterns. These results confirm the existence of advanced computational methods to diagnostic spectroscopy, which proves the presence of significant gains in clinical accuracy of non-invasive colorectal cancer screening with complex algorithms.

Conclusions

This pilot study manages to prove that gold nanoparticle-enhanced Raman spectroscopy with multivariate statistical analysis is a promising modality of non-invasive detection of colorectal cancer in blood serum. Biomolecular signatures of cancer such as increased nucleic acid concentration and reduced protein/saccharide concentration in the cancer specimen were identified in spectral analysis of 38 cancer patients and 45 healthy controls.

Two diagnostic strategies were compared, including empirical intensity ratios and all-inclusive PCA-LDA algorithms. The I 5/I 6 ratio was found to have 68.4% sensitivity and 95.6% specificity, and the PCA-LDA had 97.4% sensitivity and 100% specificity using a leave-one-out cross-validation. The analysis of ROC curves proved the outstanding performance of PCA-LDA (AUC = 1.0), which is significantly better than the empirical approach (AUC = 0.896).

These findings provide evidence of concept that SERS-based liquid biopsy can be used to screen colorectal cancer and provides the potential benefits over traditional techniques: non-invasive sampling, fast analysis, low sample volume, and objective algorithmic classification. It’s almost flawless discrimination indicates a strong potential of translation, but it must be confirmed by large-scale and multi-centered prospective clinical trials prior to clinical use. The standardization protocols, inter-

laboratory reproducibility, and performance in a variety of patient groups and disease stages should be considered in future research.

References

Sung H, Ferlay J, Siegel RL, Laversanne M, Soerjomataram I, Jemal A, Bray F. Global cancer statistics 2020: GLOBOCAN estimates of incidence and mortality worldwide for 36 cancers in 185 countries. CA Cancer J Clin, 2021;71(3):209-249.

Bray F, Ferlay J, Soerjomataram I, Siegel RL, Torre LA, Jemal A. Global cancer statistics 2018: GLOBOCAN estimates of incidence and mortality worldwide for 36 cancers in 185 countries. CA Cancer J Clin, 2018;68(6):394-424.

Siegel RL, Miller KD, Fuchs HE, Jemal A. Cancer statistics, 2022. CA Cancer J Clin, 2022;72(1):7-33.

Morgan E, Arnold M, Gini A, Lorenzoni I, Cabasag CJ, Laversanne M, Bray F. Global burden of colorectal cancer in 2020 and 2040: incidence and mortality estimates from GLOBOCAN. Gut, 2023;72(2):338-349.

Dekker E, Tanis PJ, Vleugels JLA, Kasi PM, Wallace MB. Colorectal cancer. Lancet, 2019;394(10207):1467-1480.

Benson AB, Venook AP, Al-Hawary MM, Arain MA, Chen YJ, Ciombor KK, Cohen S, et al. NCCN guidelines insights: colon cancer, version 2.2018. J Natl Compr Canc Netw, 2018;16(4):359-369.

Gandaglia G, Abdollah F, Schiffmann J, Trudeau V, Shariat SF, Kim SP, Karakiewicz PI. Distribution of metastatic sites in patients with prostate cancer: a population-based analysis. Prostate, 2014;74(2):210-216.

Lee JK, Liles EG, Bent S, Levin TR, Corley DA. Accuracy of fecal immunochemical tests for colorectal cancer: systematic review and meta-analysis. Ann Intern Med, 2014;160(3):171-181.

Navarro S, Suárez M, Castillo J, González del Rey A, Martínez-Bauer G, Balaguer F. Colorectal cancer screening: strategies to improve uptake and positive outcomes. Gastroenterol Hepatol, 2022;45(5):393-402.

US Preventive Services Task Force. Screening for colorectal cancer: US Preventive Services Task Force recommendation statement. JAMA, 2021;325(19):1965-1977.

Shaukat A, Kahi CJ, Burke CA, Rabeneck L, Sauer BG, Rex DK. ACG clinical guidelines: colorectal cancer screening 2021. Am J Gastroenterol, 2021;116(3):458-479.

Rabeneck L, Paszat LF, Hilsden RJ, Saskin R, Leddin D, Grunfeld E, Wai E, Goldwasser M, Sutradhar R, Stukel TA. Bleeding and perforation after outpatient colonoscopy and their risk factors in usual clinical practice. Gastroenterology, 2008;135(6):1899-1906.

Gellad ZF, Weiss JE, Provenzale D. Colorectal cancer screening. Clin Gastroenterol Hepatol, 2007;5(8):912-921.

Lieberman DA, Rex DK, Winawer SJ, Giardiello FM, Johnson DA, Levin TR. Guidelines for colonoscopy surveillance after screening and polypectomy: a consensus update by the US Multi-Society Task Force on Colorectal Cancer. Gastroenterology, 2012;143(3):844-857.

Niedermaier T, Balavarca Y, Brenner H. Stage-specific sensitivity of fecal immunochemical tests for detecting colorectal cancer: systematic review and meta-analysis. Am J Gastroenterol, 2020;115(1):56-69.

Chen Y, Lin D, Lin B, Qiu H, Lin J, Wu Y, Feng S. Rapid identification of benign and malignant colorectal polyps using serum surface-enhanced Raman spectroscopy combined with multivariate statistical analysis. Spectrochim Acta A Mol

Biomol Spectrosc, 2025;325:125089.
Munteanu I, Gaman C, Hermenean A, Dinischiotu A, Oprea OC. An overview of Raman spectroscopy application in cancer detection. Biosensors (Basel), 2022;12(9):704.
Krafft C, Popp J. The many facets of Raman spectroscopy for biomedical analysis. Anal Bioanal Chem, 2015;407(3):699-717.
Santos IP, Barroso EM, Bakker Schut TC, Caspers PJ, van Lanschot CGF, Choi DH, van der Kamp MF, Smits RWH, van Doorn R, Verdijk RM, Hegt VN, von der Thüsen JH, van Dekken H, Koolen MGJ, Osse EM, Mast H, Stoop H, van Doorn HC, Bonnier F, Puppels GJ, Baatenburg de Jong RJ, Koljenović S, Jaddoe VWV. Raman spectroscopy for cancer detection and cancer surgery guidance: translation to the clinics. Analyst, 2017;142(17):3025-3047.
Butler HJ, Ashton L, Bird B, Cinque G, Curtis K, Dorney J, Esmonde-White K, Fullwood NJ, Gardner B, Martin-Hirsch PL, Walsh MJ, McAinsh MR, Stone N, Martin FL. Using Raman spectroscopy to characterize biological materials. Nat Protoc, 2016;11(4):664-687.
Ferraro JR, Nakamoto K, Brown CW. Introductory Raman spectroscopy, 2nd edition. Academic Press, 2003.
Jones RR, Hooper DC, Zhang L, Wolverson D, Valev VK. Raman techniques: fundamentals and frontiers. Nanoscale Res Lett, 2019;14(1):231.
Long DA. Raman spectroscopy. McGraw-Hill, New York, 1977.
Le Ru E, Etchegoin P. Principles of surface-enhanced Raman spectroscopy and related plasmonic effects. Elsevier, 2009.
Schlücker S. Surface-enhanced Raman spectroscopy: concepts and chemical applications. Angew Chem Int Ed Engl, 2014;53(19):4756-4795.
Sharma B, Frontiera RR, Henry AI, Ringe E, Van Duyne RP. SERS: materials, applications, and the future. Mater Today, 2012;15(1-2):16-25.
Bell SEJ, Charron G, Cortés E, Kneipp J, de la Chapelle ML, Langer J, Procházka M, Tran V, Schlücker S. Towards reliable and quantitative surface-enhanced Raman scattering (SERS): from key parameters to good analytical practice. Angew Chem Int Ed Engl, 2020;59(14):5454-5462.
Guerrini L, Alvarez-Puebla RA. Cancer-associated metabolites as biomarkers for early detection: usefulness of SERS spectroscopy. Cancers (Basel), 2019;11(6):748.
Langer J, Jimenez de Aberasturi D, Aizpurua J, Alvarez-Puebla RA, Auguié B, Baumberg JJ, Bazan GC, Bell SEJ, Boisen A, Brolo AG, Choo J, Cialla-May D, Deckert V, Fabris L, Faulds K, García de Abajo FJ, Goodacre R, Graham D, Haes AJ, Haynes CL, Huck C, Itoh T, Käll M, Kneipp J, Kotov NA, Kuang H, Le Ru EC, Lee HK, Li JF, Ling XY, Maier SA, Mayerhöfer T, Moskovits M, Murakoshi K, Nam JM, Nie S, Ozaki Y, Pastoriza-Santos I, Perez-Juste J, Popp J, Pucci A, Reich S, Ren B, Schatz GC, Shegai T, Schlücker S, Tay LL, Thomas KG, Tian ZQ, Van Duyne RP, Vo-Dinh T, Wang Y, Willets KA, Xu C, Xu H, Xu Y, Yamamoto YS, Zhao B, Liz-Marzán LM. Present and future of surface-enhanced Raman scattering. ACS Nano, 2020;14(1):28-117.
Lin D, Feng S, Pan J, Chen Y, Lin J, Chen G, Xie S, Zeng H, Chen R. Colorectal cancer detection by gold nanoparticle based surface-enhanced Raman spectroscopy of blood serum and statistical analysis. Opt Express, 2011;19(14):13565-13577.
Feng S, Chen R, Lin J, Pan J, Chen G, Li Y, Cheng M, Huang Z, Chen J, Zeng H. Nasopharyngeal cancer detection based on blood plasma surface-enhanced Raman spectroscopy and multivariate analysis. Biosens Bioelectron, 2010;25(11):2414-2419.
Movasaghi Z, Rehman S, Rehman IU. Raman spectroscopy of biological tissues. Appl Spectrosc Rev, 2007;42(5):493-541.

Stone N, Kendall C, Smith J, Crow P, Barr H. Raman spectroscopy for identification of epithelial cancers. Faraday Discuss, 2004;126:141-157.
De Gelder J, De Gussem K, Vandenabeele P, Moens L. Reference database of Raman spectra of biological molecules. J Raman Spectrosc, 2007;38(9):1133-1147.
Spiro TG. Biological applications of Raman spectroscopy. Wiley, 1987.
Schulz H, Baranska M. Identification and quantification of valuable plant substances by IR and Raman spectroscopy. Vib Spectrosc, 2007;43(1):13-25.
Stone N, Kendall C, Shepherd N, Crow P, Barr H. Near-infrared Raman spectroscopy for the classification of epithelial pre-cancers and cancers. J Raman Spectrosc, 2002;33(7):564-573.
Krafft C, Neudert L, Simat T, Salzer R. Near infrared Raman spectra of human brain lipids. Spectrochim Acta A Mol Biomol Spectrosc, 2005;61(7):1529-1535.
Chan JW, Taylor DS, Zwerdling T, Lane SM, Ihara K, Huser T. Micro-Raman spectroscopy detects individual neoplastic and normal hematopoietic cells. Biophys J, 2006;90(2):648-656.
Farquharson S, Shende C, Inscore FE, Maksymiuk P, Gift A. Analysis of 5-fluorouracil in saliva using surface-enhanced Raman spectroscopy. J Raman Spectrosc, 2005;36(3):208-212.
Stone N, Kendall C, Smith J, Crow P, Barr H. Raman spectroscopy for identification of epithelial cancers. Faraday Discuss, 2004;126:141-157.
Ruiz-Chica AJ, Medina MA, Sánchez-Jiménez F, Ramírez FJ. Characterization by Raman spectroscopy of conformational changes on guanine-cytosine and adenine-thymine oligonucleotides induced by aminooxy analogues of spermidine. J Raman Spectrosc, 2004;35(2):93-100.
Frank CJ, McCreery RL, Redd DC. Raman spectroscopy of normal and diseased human breast tissues. Anal Chem, 1995;67(5):777-783.
Gniadecka M, Wulf HC, Mortensen NN, Nielsen OF, Christensen DH. Diagnosis of basal cell carcinoma by Raman spectroscopy. J Raman Spectrosc, 1997;28(2-3):125-129.
Cheng WT, Liu MT, Liu HN, Lin SY. Micro-Raman spectroscopy used to identify and grade human skin pilomatrixoma. Microsc Res Tech, 2005;68(2):75-79.
Huang Z, McWilliams A, Lui H, McLean DI, Lam S, Zeng H. Near-infrared Raman spectroscopy for optical diagnosis of lung cancer. Int J Cancer, 2003;107(6):1047-1052.
Huang Z, Lui H, McLean DI, Korbelik M, Zeng H. Raman spectroscopy in combination with background near-infrared autofluorescence enhances the in vivo assessment of malignant tissues. Photochem Photobiol, 2005;81(5):1219-1226.
Naumann D. Infrared spectroscopy in microbiology. Encyclopedia of Analytical Chemistry, 2000.
Turkevich J, Stevenson PC, Hillier J. A study of the nucleation and growth processes in the synthesis of colloidal gold. Discuss Faraday Soc, 1951;11:55-75.
Shetty G, Kendall C, Shepherd N, Stone N, Barr H. Raman spectroscopy: elucidation of biochemical changes in carcinogenesis of oesophagus. Br J Cancer, 2006;94(10):1460-1464.
Andrus PG, Strickland RD. Cancer grading by Fourier transform infrared spectroscopy. Biospectroscopy, 1998;4(1):37-46.
Bonnier F, Brachet G, Duong R, Sojinrin T, Respaud R, Aubrey N, Baker MJ, Byrne HJ, Chourpa I. Screening the low molecular weight fraction of human serum using ATR-IR spectroscopy. J Biophotonics, 2016;9(10):1085-1097.
Dukor RK. Vibrational spectroscopy in the detection of cancer. Handbook of Vibrational Spectroscopy, 2006.
Faolain EO, Hunter MB, Byrne JM, Kelehan P, McNamara M, Byrne HJ, Lyng FM. A

study examining the effects of tissue processing on human tissue sections using vibrational spectroscopy. Vib Spectrosc, 2005;38(1-2):121-127.
Wood BR, Quinn MA, Tait B, Ashdown M, Hislop T, Romeo M, McNaughton D. FTIR microspectroscopic study of cell types and potential confounding variables in screening for cervical malignancies. Biospectroscopy, 1998;4(2):75-91.
Takeuchi H. Raman structural markers of tryptophan and histidine side chains in proteins. Biopolymers, 2003;72(5):305-317.
Kaushik D, Michniak-Kohn B. Percutaneous penetration modifiers and formulation effects. Int J Pharm, 2010;386(1-2):42-51.
Nawaz H, Bonnier F, Knief P, Howe O, Lyng FM, Meade AD, Byrne HJ. Evaluation of the potential of Raman microspectroscopy for prediction of chemotherapeutic response to cisplatin in lung adenocarcinoma. Analyst, 2010;135(12):3070-3076.
Jannasch F, Bedu-Addo G, Schulze MB, Mockenhaupt FP, Danquah I. Serum lipid changes during pregnancy and risk of hypertensive disorders: a prospective study in rural Ghana. Nutr J, 2017;16(1):63.